

(43), this maximum  $\rho_0$  equals  $(b+1)\rho_0/2b^{\frac{1}{2}}$ , for which<sup>35</sup> the radicand in (47) vanishes; and the positive and negative signs, corresponding to the sign of  $\lambda$ , are to be taken in (47) for  $W_0$  respectively to the extrinsic and near-intrinsic sides of this maximum in  $\rho_0$ .

The ambipolar diffusivity  $D_0$  and group mobility  $\mu_0^*$  may be written as

$$D_0 = 2 \cosh W_0 / [D_p^{-1} \exp(W_0) + D_n^{-1} \exp(-W_0)], \quad (49)$$

and

$$\mu_0^* = 2 \sinh W_0 / [\mu_p^{-1} \exp(W_0) + \mu_n^{-1} \exp(-W_0)]. \quad (50)$$

<sup>35</sup> The corresponding  $W_0$  is  $-\ln b^{\frac{1}{2}}$ , for which  $M_s$  is  $2b/(b-1)$ , or, for germanium, about 3.8, with  $\rho_0 = 50$  ohm-cm at 300°K.

In Fig. 5,  $D_0$  and  $\mu_0^*$  are plotted against  $W_0$  for germanium at various temperatures. The quantity  $D_0^{-\frac{1}{2}}\mu_0^*$  multiplied by  $\tau_0^{\frac{1}{2}}$  gives the reciprocal of the scalar field intensity  $v_D/\mu_0^*$ , the unitary field for the dimensionless equation (36).

We should like to acknowledge our indebtedness to F. J. Morin, who has kindly made available results from an experimental investigation of germanium prior to publication; to W. Shockley, S. Millman, and W. G. Pfann for helpful suggestions; and to Miss C. L. Froelich and her staff, who have performed computations for the figures.

## The Energy Loss of Hydrogen, Helium, Nitrogen, and Neon Ions in Gases\*

PETER K. WEYL

*Department of Physics and Institute for Nuclear Studies, University of Chicago, Chicago, Illinois*

(Received March 23, 1953)

The rate of loss of energy of protons, deuterons, helium, nitrogen, and neon ions in the energy range of 150 to 450 kev has been measured in the gases hydrogen, helium, air, and argon. The ions were sent through a differentially pumped gas system and the energy loss in the forward direction due to the gas was determined with an electrostatic analyzer.

The results for protons agree with recent measurements at the California Institute of Technology. At the same energy, the stopping cross sections are roughly the same for neon and helium ions. The stopping power for nitrogen ions is greater than that for neon ions of the same energy by a factor ranging from 1.3 to 1.9, illustrating the importance of external electron configurations in determining stopping powers in our energy region. With the exception of hydrogen gas, the cross sections for the heavier ions follow a power law. The dependence ranges from  $E^{0.33}$  to  $E^{0.69}$ , depending on the gas and ion, with several of the curves following an  $E^{\frac{1}{2}}$  power law.

### I. INTRODUCTION

FOR many experiments in nuclear physics it is important to know the rate of energy loss of charged particles in matter. Recently Taylor<sup>1</sup> has reviewed the field of energy loss and range energy relations. Since this review, Kahn<sup>2</sup> of this laboratory has measured the energy loss of protons from 500–1300 kev in various metals and mica.

The energy loss of protons in gases has recently been measured in several laboratories. At Los Alamos, Phillips<sup>3</sup> has measured the energy loss of protons from 10–80 kev in H<sub>2</sub>, He, N<sub>2</sub>, O<sub>2</sub>, A, Kr, H<sub>2</sub>O, and CCl<sub>4</sub>. At the California Institute of Technology, Reynolds, Dunbar, Wenzel, and Whaling<sup>4</sup> have investigated the energy loss of protons from 25–550 kev in the gases H<sub>2</sub>, He, N<sub>2</sub>, O<sub>2</sub>, air, A, Ne, CH<sub>4</sub>, C<sub>2</sub>H<sub>2</sub>, C<sub>2</sub>H<sub>4</sub>, C<sub>2</sub>H<sub>6</sub>, H<sub>2</sub>O, NH<sub>3</sub>, NO, CO<sub>2</sub>, and N<sub>2</sub>O.

In the present investigation the energy loss of protons

from 40–450 kev in air and argon was measured. The fact that a differentially pumped gas chamber was used made it possible to measure the energy loss of heavier ions. The stopping power of H<sub>2</sub>, He, air, and A was investigated in the energy range from 150–450 kev for helium, nitrogen, and neon ions.

### II. APPARATUS

#### A. The Source of Particles

The source of the particles was the "kevatron" (500-kev Cockcroft-Walton generator) at the Institute for Nuclear Studies, University of Chicago. The beam of particles was focused by allowing it to impinge on a quartz plate and observing the fluorescence and incandescence produced. (See Fig. 1.) Next, the beam underwent a 15-degree magnetic analysis in order to separate out the ionic component desired. The arc source was of the low voltage capillary type described elsewhere.<sup>5</sup> By changing the gas admitted to the arc, singly charged ions of hydrogen, deuterium, helium, nitrogen, and neon were obtained. The ion stream also contained

\* Supported in part by the U. S. Atomic Energy Commission.

<sup>1</sup> A. E. Taylor, Repts. Progr. Phys. **15**, 49 (1952).

<sup>2</sup> D. Kahn, Phys. Rev. **90**, 503 (1953).

<sup>3</sup> J. A. Phillips (to be published).

<sup>4</sup> Reynolds, Dunbar, Wenzel, and Whaling, Bull. Am. Phys. Soc. **27**, No. 6, 6 (1952). Details of experiment to be published.

<sup>5</sup> S. K. Allison, Rev. Sci. Instr. **19**, 291 (1948).

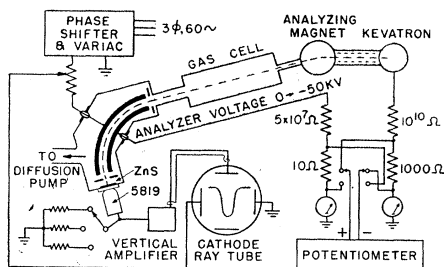


Fig. 1. General diagram of the apparatus.

several molecular ions and ions due to impurities which were eliminated by the magnetic analysis. In order to obtain low energy deuterons it was convenient to use the  $D_2^+$  beam which splits into two atomic ions of half the  $D_2^+$  energy upon encountering the gas.

### B. The Gas System

In order to avoid the use of foils, a differentially pumped gas cell was employed. Figure 2 shows the arrangement of this system. The gas cell proper was a  $76.505 \pm 0.005$ -cm long  $\frac{7}{8}$ -inch (2.22-cm) i.d. brass tube. The ends of this tube were sealed by two disks which had a No. 78 hole (0.40-mm diameter) drilled through their center. Near the hole, the disks were thinned out to 0.25 mm. This tube was mounted concentrically in a  $2\frac{1}{8}$  inches (5.40-cm) o.d. brass tube which extended 1.87 cm beyond the gas cell at each end. This tube was sealed by plates with a No. 70 hole (0.71-mm diameter) and was pumped by a 33.4-liter/min Welch Duo-Seal vacuum pump. In order to keep oil vapors out of the system, a dry ice trap was interposed between the pump and the tube. To each end of the  $2\frac{1}{8}$ -inch tube was connected a 3-inch (7.62-cm) long piece of tube terminated by a disk with a No. 60 hole (1.01-mm diameter). This section was evacuated by a 200-liter/sec diffusion pump.

The gas was admitted to the central chamber through a specially constructed needle valve, after first having passed through an appropriately filled cooling trap. The refrigerant used in this trap was identical to that in the trap protecting the McLeod gauge, so that any impurities that would be condensed in the latter trap could not enter the system.

With the above described gas system, the pressure in the forepumped section was about 10 percent of the pressure in the gas cell. The vacuum in the kevatron or the electrostatic analyzer was not noticeably affected by the presence of gas in the cell.

After getting unreliable results with various oil manometers, a McLeod gauge was used for the pressure measurement. The gauge was a Distillation Products type MG-07 triple range McLeod gauge having scales of 0-5, 0-0.5 and 0-0.05 mm of mercury. The gauge was calibrated and the calibration for the 5-mm and 0.5-mm scales agreed within 1.5 percent with the scales

supplied by the manufacturer. The 0.05 scale was replaced by a millimeter scale and a calibration curve of millimeters *versus* pressure was constructed from the calibration data.

### C. The Electrostatic Analyzer

In order to measure the energies of the ions, a cylindrical, electrostatic analyzer of 25.400-cm mean radius was used.<sup>6</sup> The constant of this analyzer was  $19.77 \pm 0.11$ . This means that the energy of an ion having  $Z$  charges and an energy  $E$  (in electron volts) traverses the analyzer if the analyzer voltage is  $E/(Z \times 19.77)$ . The analyzer constant was determined by calibrating it against a precise cylindrical analyzer<sup>7</sup> whose constant was known both by calculation from the dimensions and from direct electrical calibration. The entrance and exit of the analyzer were defined by 1-mm slits. The exit to the analyzer was closed by a glass disk. The inside of this disk was covered by a thin layer of silicone grease and then dusted with fluorescence ZnS crystals (Fluorescent-2205, New Jersey Zinc Company).

A type 5819 RCA photoelectron multiplier tube was placed against the outer surface of the glass disk to detect the scintillations caused by the ions hitting the ZnS crystals. The phototube was powered by a vacuum tube regulated power supply. The vacuum of the analyzer was maintained by a separate diffusion pump and watched by an ionization gauge.

The deflecting voltage for the electrostatic analyzer was supplied by a 50-kv voltage doubler circuit of conventional design.<sup>8</sup> The analyzer voltage was determined by measuring the current drain through a 50-megohm precision resistor stack in parallel with the analyzer plate. The stack was in series with a 10-ohm precision resistor, and a potentiometer (Rubicon type 2703) was used to measure the voltage drop across this resistor.

A modulation technique was used in order to make the energy analysis independent of the beam fluctuations. The 0.40-mm diameter entrance aperture to the absorption cell was so small that fluctuations of intensity within the focal spot of the beam affected the current through the gas cell. As these fluctuations were fairly slow, the analyzer was swept through the energy spectrum at 60 cycles. This was accomplished by applying a 250-volt rms 60-cycle sine wave to the normally grounded plate of the analyzer. The same modulating voltage was applied directly to the horizontal deflection plates of a Dumont type 208-B cathode-ray oscilloscope (see Fig. 1). Thus the instantaneous modulating signal was plotted linearly along the  $X$  axis of the cathode-ray tube. As the modulating

<sup>6</sup> Allison, Skaggs, and Smith, *Phys. Rev.* **54**, 71 (1938).

<sup>7</sup> Allison, Frankel, Hall, Montague, Morrish, and Warshaw, *Rev. Sci. Instr.* **20**, 735 (1949).

<sup>8</sup> The 0-50-kv dc power supply model No. 2008 was manufactured by the Beta Electric Corporation, New York, New York.

signal went symmetrically above and below ground potential, the undeflected spot on the cathode-ray tube corresponded to zero instantaneous modulating voltage.

The anode of the 5819 photomultiplier tube was connected to the *Y* amplifier of the CRO, and this input was shunted to ground by any one of a set of fixed resistors. The *Y* deflection was then proportional to the photomultiplier current. By changing the gain of the amplifier and the value of the fixed resistor (100 ohms to 10 megohms), it was possible to vary the amplitude of the signal. As the photomultiplier current was proportional to the number of scintillations, the scope displayed a plot of detector current *versus* bias voltage. The dc voltage on the analyzer was now adjusted until the peak of the trace corresponded to zero *X* deflection. Hence at the instant when the peak of the distribution appeared on the scope, the total analyzer voltage was given by the dc voltage. This voltage corresponds to the most probable energy (mode) of the beam. Any intensity fluctuations will change the amplitude of the distribution but not the *X* coordinate of the peak.

This simple analysis was complicated by the ripple of the kevatron. As the modulating voltage and the high voltage of the kevatron were both derived from line voltage there was a fixed phase relationship between the ripple and the modulating signal. During each cycle of the line voltage, the kevatron goes through one ripple cycle, while the analyzer sweeps through the energy spectrum twice. Thus, two peaks appear on the scope. By adjusting the phase of the modulator it was possible to make the two peaks coincide.

### III. PROCEDURE OF MEASUREMENT

A. Depending on the ion under investigation, the proper gas was admitted to the low voltage arc source. The kevatron was then set to the approximate voltage needed and the beam was focused.

B. With vacuum in the gas cell, the proper beam was deflected into it with the deflecting magnet. In the case of neon, the isotopes of mass 20 and 22 were well separated. The more abundant isotope of mass 20 was used for the measurements. The analyzer voltage was set to the proper voltage, and the beam intensity was maximized.

C. The high voltage of the kevatron was now measured by measuring the voltage across a 1000-ohm resistor which was in series with the  $10^{10}$ -ohm high voltage resistor of the kevatron. This measurement was made with a potentiometer. The potentiometer was now kept in balance by adjusting the kevatron high voltage. While the high voltage was thus stabilized, the analyzer modulation voltage phase was adjusted until only one peak showed on the scope. This peak was then lined up with a hairline defining the  $X=0$  line on the scope, by adjusting the analyzer voltage. Once the analyzer was set up, the potentiometer was

used to measure the voltage across a 10-ohm resistor in series with the 50-megohm analyzer voltage resistor. The analyzer voltage was then shifted slightly and the procedure was repeated so that at least two independent measurements of the analyzer voltage without gas were made. Next, the "vacuum" pressure in the gas cell was measured with the McLeod gauge. This pressure was usually about 2 microns.

D. Now gas was slowly admitted to the absorption cell. The pressure in the cell was watched by a thermocouple gauge, and the peak on the cathode-ray tube trace was seen to move toward lower energy. The charge of the analyzer was reduced in order to keep the trace in view. Owing to scattering of the ion beam, the amplitude of the signal was rapidly diminished. This was compensated for by increasing the gain of the *Y* amplifier, increasing the voltage on the photomultiplier tube, and switching a higher shunt resistance across the input of the *Y* amplifier. When a sufficient amount of gas had been admitted to the cell, the pressure was allowed to stabilize. Once equilibrium had been reached, the high voltage of the kevatron was again stabilized

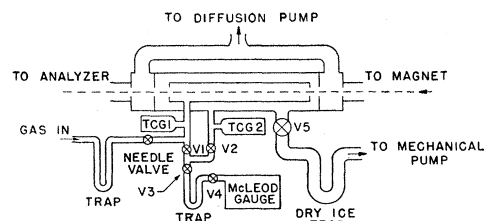


FIG. 2. The gas system.

at the preset voltage, and the analyzer voltage was set up by aligning the peak with the hairline. Owing to the presence of the gas, the peak was now considerably broadened. For heavy ions in heavy gases the peak consisted of a series of overlapping pulses. Once the analyzer was set, its voltage was measured. The peak was then set up once more and the analyzer voltage remeasured. The energy loss due to the gas was never allowed to be more than 10 percent of the beam energy.

E. Next, the pressure in the gas cell was measured with the McLeod gauge. As the laboratory was air-conditioned and the temperature never varied by more than one degree it was not necessary to take temperature readings more than twice a day. One measurement of the energy loss was now completed. Initially, the measurements were taken in the following order: First, a vacuum reading. This was followed by a reading at one pressure of gas. Then the gas pressure was changed, and a second pressure reading was made followed by another vacuum reading. The two vacuum readings usually agreed within the errors. The energy loss computed from the two pressure measurements also agreed within the errors. For the later measurements only one vacuum and one pressure measurement were made.

#### IV. ERROR ANALYSIS

The calculation of the energy loss consists of taking the difference of two potentiometer readings, dividing this by a pressure reading, and then multiplying the result by a conversion factor. The errors therefore fall into three categories.

1. *The error in the potentiometer reading.* This error is extremely important as we have to take the difference of two readings that differ only by about 10 percent. In the voltage measurement only the slidewire was adjusted for readings with and without gas. The guaranteed accuracy of the slidewire is one scale division or 0.005 mv. Kahn,<sup>2</sup> who used the same instrument, has compared it to other potentiometers and found the accuracy to be considerably better than specified by the manufacturer. The essential error depends on how accurately it is possible to set up the peak of the distribution and what the difference in energy between the two measurements is. In each run, the percentage error in the energy measurement was estimated by dividing the estimated errors in setting up the peak by the energy difference. This varied from run to run depending on the sharpness of the peaks and the total energy loss. This error ranged from 0.5 percent to 5 percent, the best results being for protons where the peaks were very sharp due to the small relative scattering.

2. *The error in the pressure measurement.* This error was due to the error in reading the McLeod gauge scale and due to the uncertainty of the calibration. The percentage error depends on the scale used and the pressure measured. For each determination this error was computed. It ranged from 0.5 percent to about three percent.

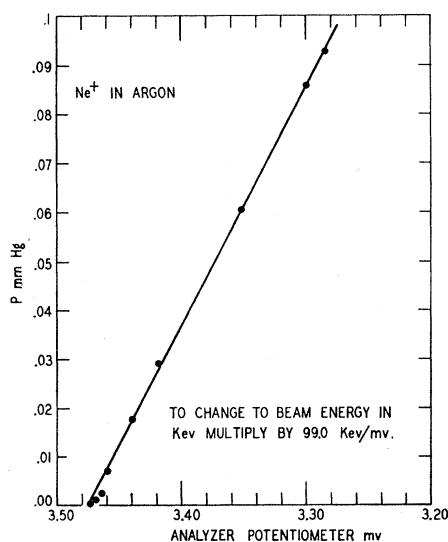


FIG. 3. Energy of the emergent beam as a function of the gas pressure in the absorption tube.

3. *The error due to the conversion factor.* In order to convert from millivolts per mm mercury to energy loss per cm at one standard atmosphere, a conversion factor has to be used. This factor is made up of the values of the standard resistors used, the analyzer constant, the effective length of the gas cell and a temperature conversion to zero degrees centigrade. The effective length of the gas cell is 0.5 percent longer than the geometrical length, due to the gas in the forepumped section of the differential pumping system. As high quality, standardized resistors were used and as the gas cell was very long, the only significant error is due to a  $\frac{1}{2}$  percent uncertainty of the analyzer constant.

4. In practice, the percentage errors due to the pressure measurement and the energy measurement were simply added. If the sum was 1.5 percent or less, the 0.5 percent error of the analyzer constant was added; otherwise, it was ignored as being negligible compared to the above errors. The smallest possible error is therefore 1.5 percent. The worst error for heavy ions at low energies amounted to about 10 percent. In the curves of the results, the errors of each measurement are indicated. In order to make sure that there were no other errors present, the emergent beam energy was measured as a function of the pressure in the gas cell over a large range of pressures. Figure 3 shows such a determination. It is seen that the energy loss is linear with pressure showing that the atomic stopping power is independent of the gas pressure. When experimental difficulties were encountered (e.g., before the use of the McLeod gauge), this test showed marked nonlinearity. This test was repeated from time to time to show that the experiment was being carried out properly.

#### V. RESULTS

The gases used in the determination were the following:

*Air.* The air used in the measurements was freed of moisture by passing it through a 3 ft long drying tube. The air was then passed through a dry ice-acetone trap before entering the gas cell.

*Argon.* The argon was obtained from a lecture bottle purchased from the Matheson Company with a purity of 99.9 percent. Care was taken to evacuate the feed line before the gas was admitted in order not to contaminate the gas with air. The traps were filled with a dry ice-acetone mixture.

*Helium.* The helium used was Bureau of Mines grade A with a quoted purity of 99.8 percent. At first, non-reproducible results were obtained due to a slight diffusion of air into the system. Due to the slow rate of gas flow and the small volume of the gas system between the pressure regulator and the needle valve, even a slow contamination rate was serious. In order to overcome this difficulty, a bubbler was installed in the system. By bubbling a steady flow of helium into the atmosphere through mercury, a continuous flow of pure

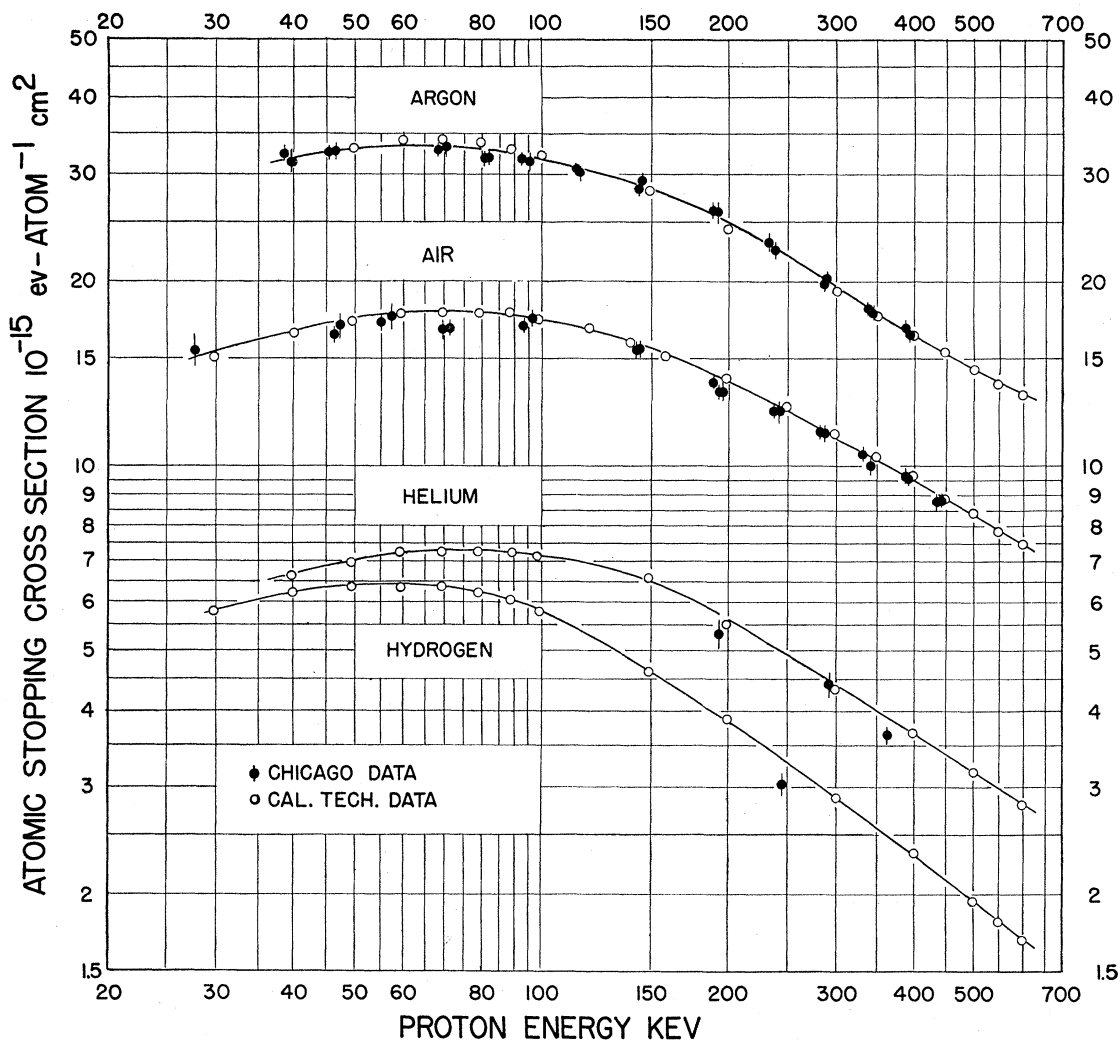


FIG. 4. The atomic stopping cross sections of several gases for protons.

helium was taken from the tank. By making this flow very large compared to the small leakage rate, the contamination of the helium was kept negligible. The helium was passed through a liquid nitrogen trap in order to freeze out moisture and other condensable vapors.

*Hydrogen.* The hydrogen used was electrolytic hydrogen which had been passed through a "Deoxo" unit and a liquid nitrogen trap in order to remove any oxygen present. The above described bubbler was also used with the hydrogen supply. The traps were filled with liquid nitrogen.

The atomic stopping power for protons is shown on Fig. 4 where the errors of each determination are indicated. The results of the California Institute of Technology measurements<sup>4</sup> kindly supplied us before publication are also shown. For hydrogen and helium only a few points were obtained and the California Institute of Technology curves are drawn. Our results

for argon and air and the California Institute data for hydrogen and helium are listed in Table I. These data represent points read off the smoothed out curves.

The atomic stopping cross sections for helium ions are shown on Fig. 5 and listed in Table I. It is seen that, with the exception of the curve in hydrogen gas, the results are well represented by a power law over the range of energies measured. The exponent is indicated on the figure.

The atomic stopping cross sections for nitrogen, and for neon ions of mass 20, are shown on Fig. 6. Again, with the exception of the hydrogen data, the stopping cross section is proportional to some power of the energy. The smoothed out values of the energy loss cross section are tabulated in Table I.

In order to give an over-all view of the various results, a plot of the stopping power per electron as a function of the square of the ion velocity is presented (Fig. 7). The data for protons above 100 kilovolts are

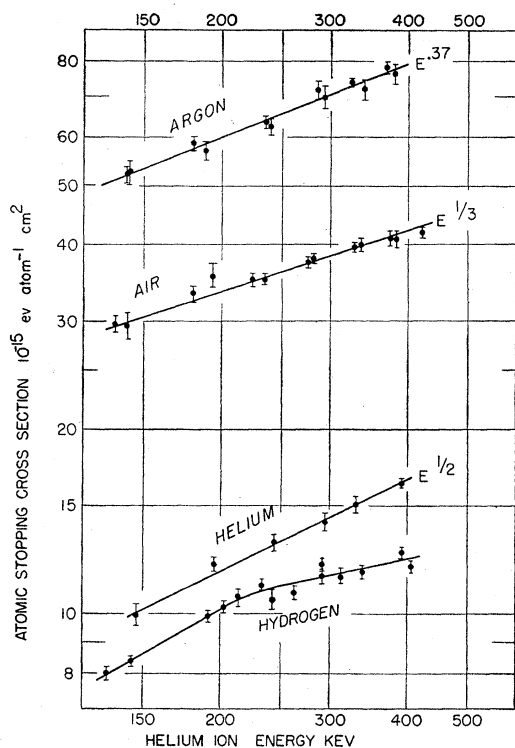


FIG. 5. The atomic stopping cross sections of several gases for helium ions.

omitted from this curve.

Table II is a list of conversion factors in order to facilitate changing the energy loss cross sections to other units.

## VI. DISCUSSION

### A. The Modes of Energy Loss

There are three principal mechanisms by which a fast ion traversing a gas loses energy.

1. *Stopping by inelastic collisions with electrons.* At energies where the ion velocities are large compared to the velocity of the orbital electrons, this mechanism accounts for practically all the stopping. In this energy range, the theory by Bethe<sup>9</sup> based on a Born approximation calculation gives the well-known formula for the differential energy loss due to this mechanism. However, for the ion energies under investigation, this formula is not applicable. As the ions are moving with velocities comparable to those of the orbital electrons, a calculation of the electronic stopping power becomes extremely complicated.

2. *Stopping by charge exchange.* When a slow ion traverses a gas, its charge is not constant. The ion continually picks up and loses electrons. The net effect of one capture-loss cycle is that one atom of the gas has been ionized. Hence, the ion must have lost at

least an energy equal to the first ionization potential of the gas.

The charge exchange of protons in hydrogen and air has been studied in this laboratory by Montague, Ribe, and Kanner.<sup>10</sup> The ratio of the charge states of helium ions in gases has been studied by Snitzer.<sup>11</sup>

The data on protons allow us to put a lower limit on the energy loss due to charge exchange. We shall calculate this loss in hydrogen (and air) at an energy where the electron capture and loss cross sections are equal. This turns out to be 52 (25) kev. At this energy the cross sections are  $6.3(24) \times 10^{-17}$  cm<sup>2</sup>. Since only one-half the ions at this energy are singly charged and can pick up an electron, we have to divide the above cross section by two. Multiplying this by the ionization potential, we get  $0.49(1.8) \times 10^{-15}$  cm<sup>2</sup> ev/atom, which is the lower limit for the energy loss due to charge

TABLE I. Atomic energy loss cross section in units of  $10^{-15}$  ev cm<sup>2</sup> atom<sup>-1</sup>.<sup>a</sup>

Particle	E(kev)	Gas			
		Hydrogen	Helium	Air	Argon
Proton	30	5.84	...	15.5	...
	40	6.25	6.67	16.5	32
	50	6.43	6.97	17.5	33
	75	6.3	7.35	18	33
	100	5.83	7.30	17.3	31.5
	125	5.2	6.9	6.5	30
	150	4.70	6.37	15.5	29
	175	4.2	6.0	14.5	27
	200	3.90	5.55	13.5	25.5
	250	3.33	4.91	12.3	22
	300	2.91	4.41	11.2	19.7
350	2.60	4.01	10.3	18	
400	2.35	3.69	9.6	16.5	
450	2.14	3.42	8.9		
500	1.97	3.18			
Helium ion	150	8.6	10.2	30.6	53.3
	175	9.4	11.0	43.3	57.0
	200	10.2	11.7	33.7	60.0
	250	11.0	13.2	36.3	66.0
	300	11.4	14.4	38.5	71.0
	350	11.9	15.5	40.5	75.0
400	12.3	16.7	42.3	79.0	
Nitrogen ion	150	12.7	16.7	...	...
	175	13.3	17.7	...	...
	200	13.8	18.7	52.6	90
	250	15.2	20.5	59.0	102
	300	17.0	22.2	64.5	114
	350	17.7	23.7	70.0	125
400	18.5	25.0	74.5	135	
Neon-20 ion	150	...	10.5	...	...
	175	6.9	11.8	...	...
	200	7.3	12.8	41	63
	250	7.9	14.3	46	70
	300	8.8	16.0	50.5	77
	350	9.6	17.5	54.5	83
400	10.3	18.0	58	86	

<sup>a</sup> The data for protons in hydrogen and helium are those of Reynolds *et al.* (reference 3).

<sup>10</sup> J. H. Montague, Phys. Rev. **81**, 1026 (1951); F. L. Ribe, Phys. Rev. **83**, 1217 (1951); H. Kanner, Phys. Rev. **84**, 1211 (1951).

<sup>11</sup> E. Snitzer, Phys. Rev. **89**, 1237 (1953).

<sup>9</sup> H. A. Bethe, Ann. Physik **5**, 325 (1930).

exchange. By comparison, the total measured energy loss cross section is  $6.4(14) \times 10^{-15} \text{ cm}^2 \text{ ev/atom}$ . Hence the charge exchange phenomenon accounts for at least 7.7 (13) percent of the stopping power. At higher ion velocities the electron capture cross section decreases rapidly, and therefore the effect of charge exchange becomes negligible. Unfortunately no data are as yet available to give an estimate of the contribution of charge exchange to the stopping of heavier ions. It is expected, however, that the effect will be even more important than for protons. We can conclude, therefore, that any theory which hopes to give a reasonable estimate of the stopping power found in this experiment must evaluate the energy loss due to charge exchange in addition to the loss from electronic collisions.

3. *Elastic nuclear collisions.* When a particle is scattered by the nuclear coulomb field of a gas atom, the atom recoils, taking away part of the energy. If the particle is scattered through an angle  $\theta$ , conservation of energy and momentum requires that the energy

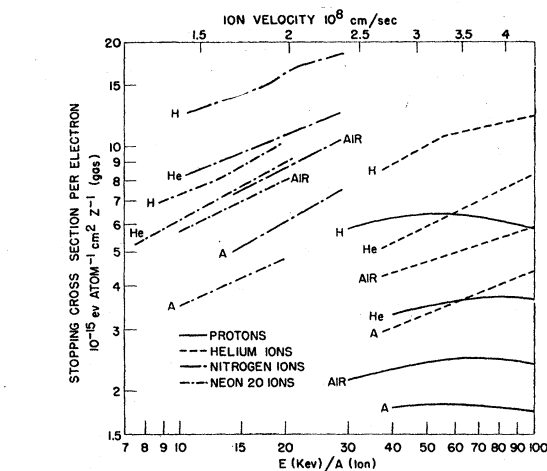


FIG. 7. The stopping cross section per electron as a function of the ion velocity.

loss be

$$\Delta E = E_p \theta^2 M_p / M_a \quad \text{for } \theta < 1,$$

where  $E_p$  and  $M_p$  are the energy and mass of the particle and  $M_a$  is the mass of the gas atom. Bohr<sup>12</sup> has integrated this loss over all angles for a screened nuclear field and finds the atomic energy loss cross section by

TABLE II. Conversion factors for expressing stopping power in various units.

Given units	Units desired			
	(kev X cm <sup>2</sup> )	(ev X cm <sup>2</sup> )	ergs/cm at NTP*	kev/cm at NTP
(kev X cm <sup>2</sup> )	H <sub>2</sub> 1	1.673 X 10 <sup>-18</sup>	1.440 X 10 <sup>-10</sup>	0.0899
	He 1	6.645	2.881 X 10 <sup>-10</sup>	0.1786
	Air 1	24.05	2.070 X 10 <sup>-9</sup>	1.293
	Argon 1	66.29	2.855 X 10 <sup>-9</sup>	1.782
(ev X cm <sup>2</sup> )	5.977 X 10 <sup>17</sup>	H <sub>2</sub> 1	8.610 X 10 <sup>7</sup>	5.375 X 10 <sup>16</sup>
	1.505	He 1	4.305	2.688
	0.4158	Air 1	8.610	5.375
	0.1508	Argon 1	4.305	2.688
erg/cm at NTP	69.42 X 10 <sup>8</sup>	1.162 X 10 <sup>-8</sup>	H <sub>2</sub> 1	6.243 X 10 <sup>8</sup>
	34.95	2.323	He 1	6.243
	4.828	1.162	Air 1	6.243
	3.498	2.323	Argon 1	6.243
kev/cm at NTP	11.12	1.861 X 10 <sup>-17</sup>	1.602 X 10 <sup>-9</sup>	H <sub>2</sub> 1
	5.599	3.722	1.602	He 1
	0.7734	1.861	1.602	Air 1
	0.5612	3.722	1.602	Argon 1

\* NTP means 0°C, 760 Hg.

this process to be

$$\sigma \left( \frac{dE}{dx} \right)_{\text{nuclear}} = \frac{4\pi e^4 Z_p^2 Z_a^2}{M_a v^2} \ln \frac{\mu v^2 A}{Z_1 Z_2 e^2},$$

where  $\mu = M_a M_p / (M_a + M_p)$ . The quantity  $v$  is the velocity of the particle, and  $Z_a, Z_p, M_a, M_p$  are the charge and mass of the gas atom and the particle, respectively.  $A$  is the screening distance, which is given approximately by  $A \approx a_0 (Z_a^{1/2} + Z_p^{1/2})^{-1/2}$ , where  $a_0$  is the Bohr radius.

<sup>12</sup> N. Bohr, Phys. Rev. 59, 270 (1941).

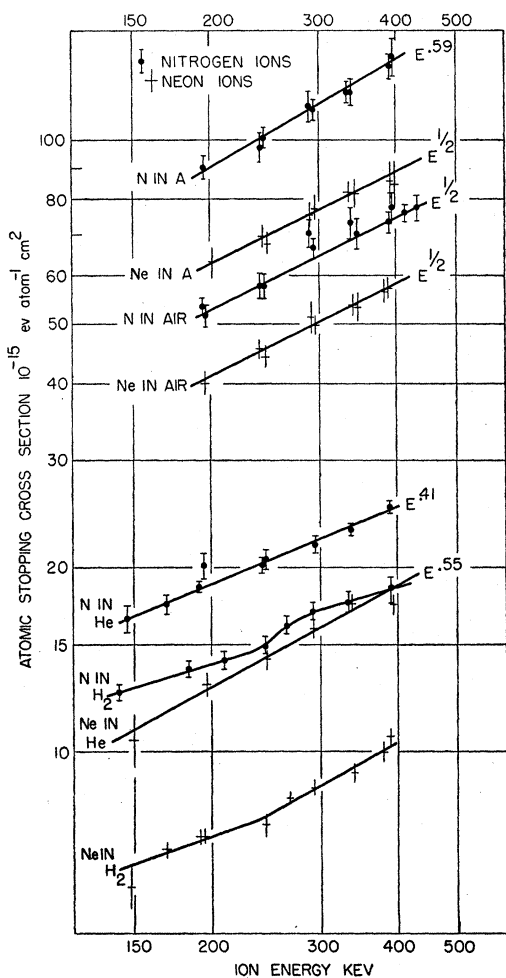


FIG. 6. The atomic stopping cross sections of several gases for nitrogen and neon ions.

We shall investigate the effect of the nuclear scattering for the extreme case, neon ions in argon gas, at  $E_p = 200$  kev. The pertinent data are:

Screening distance  $A = 1.56 \times 10^{-9}$  cm.

De Broglie wavelength  $\lambda = \hbar / (M_p v) = 2.35 \times 10^{-13}$  cm.

Distance of closest approach  $b = 2e^2 Z_a Z_p / \mu v^2 = 2.0 \times 10^{-10}$  cm.

The total nuclear energy loss cross section becomes

$$\sigma = 3.0 \times 10^{-14} \text{ cm}^2 \text{ ev/atom.}$$

For comparison, the energy loss cross section measured in this experiment is  $9 \times 10^{-14} \text{ cm}^2 \text{ ev/atom}$ .

Next we investigate the nuclear scattering contribution to the energy loss for the good geometry ( $\approx 10^{-3}$  radian) of this experiment. As the de Broglie wavelength is  $10^{-3}$  of the distance of closest approach, a classical theory of the scattering is valid. Bohr<sup>13</sup> has shown that for impact parameters larger than the screening distances, the scattering cross section decreases rapidly. The critical scattering angle ( $\theta_a$ ) where the impact parameter is equal to the screening distance is in our case  $\theta_a = 0.084$  radian. The scattering through smaller angles corresponding to larger impact parameters can be ignored. The unscreened Rutherford differential scattering cross section for small angles is

$$\begin{aligned} d\sigma(\theta)/d\theta &= 2\pi Z_a^2 Z_p^2 e^4 / E_p^2 \theta^3 \\ &= (1.06 \times 10^{-19} / \theta^3) \text{ cm}^2. \end{aligned}$$

As the critical angle is large compared to the geometry of the absorption tube, any particle which undergoes one nuclear scattering having  $\theta$  larger than  $\theta_a$  will be removed from the beam. Next, we investigate the contribution to the emergent beam due to multiply scattered ions.

The integrated scattering cross section for scattering through an angle larger than  $\theta_a$  is

$$\sigma = \int_{\theta_a}^{\infty} 1.06 \times 10^{-19} \theta^{-3} d\theta = 7.35 \times 10^{-18} \text{ cm}^2.$$

This gives a mean free path for scattering in the gas of 39 cm at a pressure of 0.1-mm Hg. The length of the tube corresponds to two mean free paths for scattering through angles larger than the critical angle. Therefore, the possibility of multiple scattering is negligible as one

scattering will cause the particle to hit the wall of the absorption tube before a second scattering can take place. We conclude that the present measurement does not contain any contribution to the energy loss due to nuclear scattering.

## B. Application of the Data

The energy loss cross sections give the most probable energy loss in the forward direction of the ion beam. Because of the lack of a theory, any extrapolations of the curves cannot be relied upon. The fact that a power law fits most of the data well is almost certainly due to the small range of energies of the present measurements and should not be assigned any great significance. If any attempt is made to use the present data to estimate the energy loss of other ions or of ions in other gases, the results must be regarded with great skepticism. The fact that the energy loss of nitrogen is larger than that of neon shows that the outer electrons strongly affect the stopping power, and hence using a simple dependence of the stopping on the atomic number will not give correct results.

For the heavier particles an integration of the stopping power will not give the range relation as the effect of nuclear stopping is not included in these measurements. Stier and Evans<sup>14</sup> have shown that nuclear stopping is of primary importance in a range determination for our region of energies and masses. It gives rise to an exponential attenuation of the beam in the forward direction and produces a wide lateral spread. For this reason the concept of range becomes rather meaningless at low ion velocities. Jorgensen<sup>15</sup> has also measured the ionization range of slow protons in several gases. He finds it necessary to use ion chambers of very large diameter in order to obtain a unique range independent of the pressure. It should be noted that these effects only become important at low ion velocities and hence the range of high energy protons and alphas is well defined.

The author wishes to thank Professor Samuel K. Allison for suggesting this problem, for extending the facilities of his laboratory, and for his constant advice and encouragement without which this work would not have been possible. Grateful acknowledgment is also made to Gordon Du Floth, Frank Sammons, and Stanley Weissman for assistance in obtaining the data.

<sup>13</sup> N. Bohr, Kgl. Danske Videnskab. Selskab, Mat.-fys. Medd. **18**, 8, Sec. 1.4 (1948).

<sup>14</sup> Stier and Evans, Phys. Rev. **88**, 164 (1952).

<sup>15</sup> T. Jorgensen (private communication).